Developmental Biology 348 (2010) 153–166

Contents lists available at ScienceDirect

Developmental Biology

journal homepage: www.elsevier.com/developmentalbiology

Notch induces cyclin-D1-dependent proliferation during a specific temporal window of neural differentiation in ES cells

Debashish Das [a,1], Fredrik Lanner [a], Heather Main [a], Emma R. Andersson [a], Olaf Bergmann [a], Cecilia Sahlgren [a], Nina Heldring [b], Ola Hermanson [b], Emil M. Hansson [a], Urban Lendahl [a,*]

[a] Department of Cell and Molecular Biology, Karolinska Institute, SE-171 77 Stockholm, Sweden
[b] Department of Neuroscience, Karolinska Institute, SE-171 77 Stockholm, Sweden

ARTICLE INFO

Article history:
Received for publication 15 February 2010
Revised 6 September 2010
Accepted 21 September 2010
Available online 29 September 2010

Keywords:
PI3 kinase
MAP kinase
Cyclin
Cell cycle
CSL
Neural induction
Jagged
Rb

ABSTRACT

The Notch signaling pathway controls cell fate choices at multiple steps during cell lineage progression. To produce the cell fate choice appropriate for a particular stage in the cell lineage, Notch signaling needs to interpret the cell context information for each stage and convert it into the appropriate cell fate instruction. The molecular basis for this temporal context-dependent Notch signaling output is poorly understood, and to study this, we have engineered a mouse embryonic stem (ES) cell line, in which short pulses of activated Notch can be produced at different stages of in vitro neural differentiation. Activation of Notch signaling for 6 h specifically at day 3 during neural induction in the ES cells led to significantly enhanced cell proliferation, accompanied by Notch-mediated activation of cyclin D1 expression. A reduction of cyclin-D1-expressing cells in the developing CNS of Notch signaling-deficient mouse embryos was also observed. Expression of a dominant negative form of cyclin D1 in the ES cells abrogated the Notch-induced proliferative response, and, conversely, a constitutively active form of cyclin D1 mimicked the effect of Notch on cell proliferation. In conclusion, the data define a novel temporal context-dependent function of Notch and a critical role for cyclin D1 in the Notch-induced proliferation in ES cells.

Introduction

Cellular differentiation is orchestrated by a surprisingly small number of signaling mechanisms, and as a consequence of this economic life style, signaling mechanisms are used reiteratively at different time points in a given cell lineage to control cell fate decisions (Hurlbut et al., 2007). To produce the appropriate signaling output for each cell fate decision, the signaling pathway must sense the cellular context at each given time point in order to provide the correct stage-specific response, but little is known about how this is accomplished during cell lineage progression.

The Notch signaling pathway is highly evolutionarily conserved and is reiteratively used in cell fate decisions in many cell lineages. Ligand activation of the membrane-bound Notch receptor ultimately leads to a cleavage of the receptor, releasing the intracellular domain of the Notch receptor (Notch ICD), which translocates to the cell nucleus (Kopan and Ilagan, 2009). In the nucleus, Notch ICD interacts with the DNA-binding protein CSL (also referred to as RBP-Jk) and converts CSL from a transcriptional repressor to an activator, which leads to activation of Notch downstream target genes, such as *Hes* and *Hey* genes (Bray, 2006). Notch signaling plays a key role in many cell lineages and is used at consecutive decision points, for example, in the developing CNS (Mizutani et al., 2007). There is also evidence that only a brief alteration of Notch signaling is sufficient to execute a particular fate decision. For example, in neural crest differentiation, a short pulse of Notch was sufficient to override BMP-mediated neurogenesis at a step upstream of MASH1 (Morrison et al., 2000). Conversely, blocking of Notch in the chick retina during Muller glia de-differentiation to progenitor cells prevents regeneration, whereas at a later stage, blocking of Notch leads to an increase in the number of new neurons (Hayes et al., 2007).

The molecular mechanisms for how Notch signaling interprets the cell context and how this modifies the signaling outputs are not well understood, and in this report, we have addressed this issue in mouse embryonic stem (ES) cells. ES cells are pluripotent cells, which can be in vitro differentiated into various lineages. The process of early neural induction has been extensively studied in ES cells (Stavridis and Smith, 2003). The early transitions are accompanied by a shift in gene expression, where pluripotency-associated genes such as *Oct4*, *Nanog*, and *SSEA1* are downregulated, followed by a transient Sox1 activation and later expression of neural progenitor markers such as nestin and BLBP. The molecular mechanisms controlling this transition are still poorly understood, but constitutive expression of Notch1 ICD in ES cells caused an accelerated entry into the neural lineage, with an earlier onset of BLBP expression (Lowell et al., 2006). This

* Corresponding author. Fax: +46 8 308374.
E-mail address: Urban.Lendahl@ki.se (U. Lendahl).
[1] Present address: Imgenex India Pvt Ltd., E-5, Infocity, KIIT Post Office, Bhubaneswar, Orissa, 751024 India.

0012-1606/$ – see front matter © 2010 Elsevier Inc. All rights reserved.
doi:10.1016/j.ydbio.2010.09.018

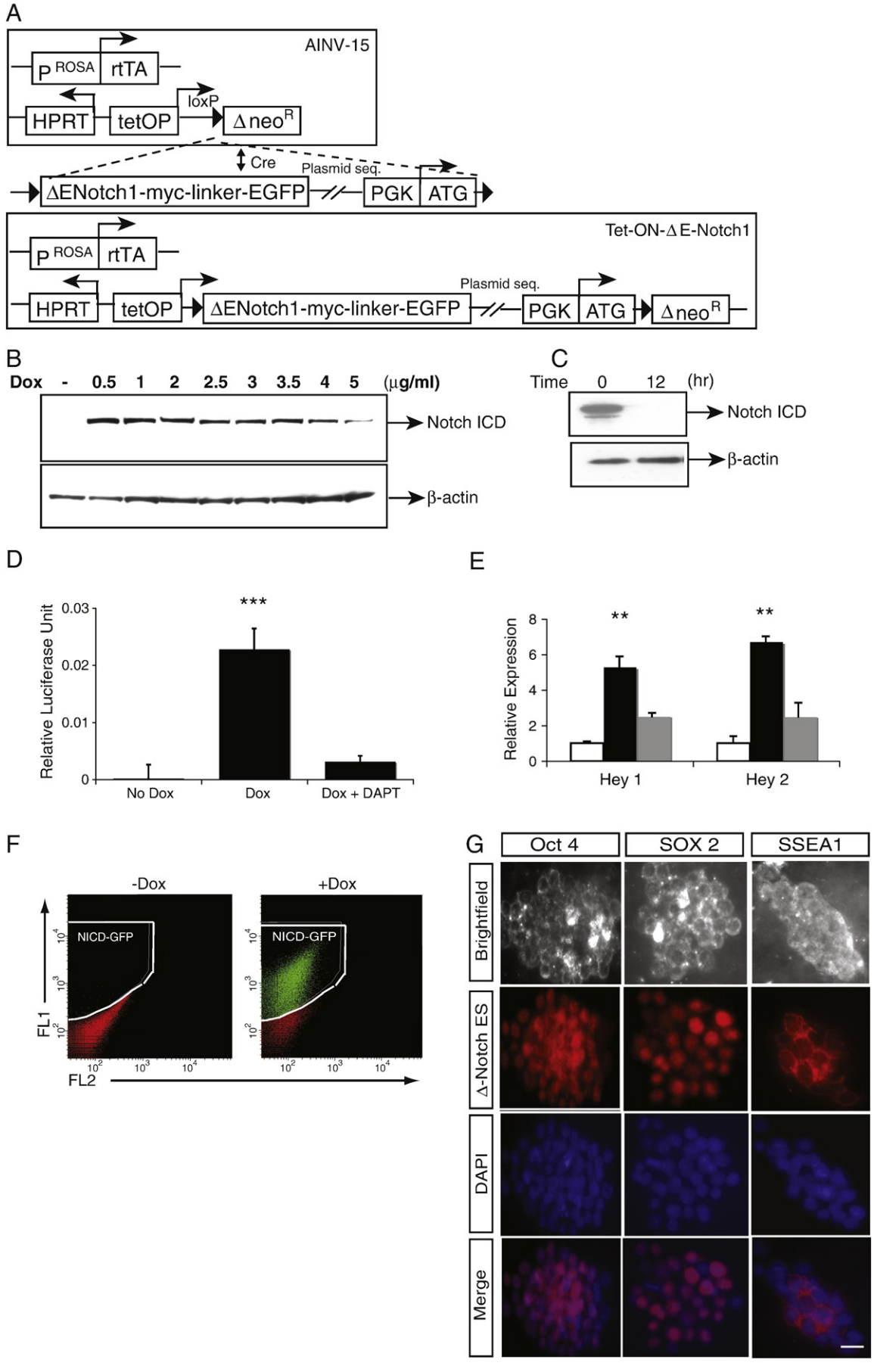
A
AINV-15
P ROSA
rtTA
HPRT
tetOP
loxP
ΔneoR
Cre
Plasmid seq.
ΔENotch1-myc-linker-EGFP
PGK
ATG
Tet-ON-ΔE-Notch1
B
Dox - 0.5 1 2 2.5 3 3.5 4 5 (μg/ml)
Notch ICD
β-actin
C
Time 0 12 (hr)
Notch ICD
β-actin
D
Relative Luciferase Unit
0.03
0.02
0.01
0
***
No Dox
Dox
Dox + DAPT
E
Relative Expression
8
6
4
2
0
**
**
Hey 1
Hey 2
F
-Dox
+Dox
NICD-GFP
NICD-GFP
FL1
FL2
G
Oct 4
SOX 2
SSEA1
Brightfield
Δ-Notch ES
DAPI
Merge

suggests that Notch plays a role in the neural differentiation process and that the effects of charging the cells with a precise temporal activation of Notch may provide insights into the temporal context-dependent control of signaling output.

In this report, we have studied the effects of short pulses of Notch signaling at different stages of early neural differentiation in ES cells. The data identify a novel temporal-context-dependent Notch function, where Notch caused an increased level of proliferation when activated specifically at day 3 in the early neural differentiation process. This proliferative burst was accompanied by upregulation of cyclin D1 by Notch, and cyclin D1 was pivotal for executing the Notch-induced proliferation, thus linking Notch directly to G1/S cell cycle transition control in this process. The data provide new insights into a role for Notch in ES cell proliferation and cell cycle control and unveil a previously unrecognized temporal window during early stages of neural differentiation.

Materials and methods

Generation of the Notch1ΔE^{TetOn} cell line

A cDNA encoding mouse Notch1ΔE (a kind gift from Dr. Raphael Kopan), a membrane-tethered form of mouse Notch1 that is a constitutive substrate for the γ-secretase complex, was subcloned to a vector encoding a multimerized glycine–serine linker and EGFP (a kind gift from Dr. Shahragim Tajbakhsh), resulting in a cDNA cassette encoding Notch1ΔE-EGFP. This cDNA was subsequently subcloned into the plox vector to generate plox-Notch1ΔE-EGFP. AINV15 cells were co-transfected with plox-Notch1ΔE-EGFP and CMV-Cre, and following selection in G418, individual clones were picked and analyzed for integration of the Notch1ΔE-EGFP cassette into the loxP site immediately 3′ of a tetracycline-controlled promoter in the HPRT locus by PCR. Two clones, #1 and #5, of the resulting cell line (Notch1ΔE^{TetOn}) were expanded for further analysis. In the pAINV-15 cell line, the gene of interest is placed under control of a tetracycline-responsive element in the HPRT locus, with the reverse tetracycline transactivator (rtTA) constitutively expressed from the Rosa26 locus. The plox vector and AINV15 cells were a kind gift from Drs. Michael Kyba and George Daley (Kyba et al., 2002).

Antibodies and pharmacological blockers

The primary antibodies used in this study were monoclonal anti-cleaved Notch1 (Cell Signaling), polyclonal anti-cyclin D1 (Santa Cruz Bio.), polyclonal anti-Oct4 (Santa Cruz Bio.), monoclonal anti-SOX2 (Abcam), monoclonal anti-SSEA-1 (Abcam), monoclonal anti-beta actin (Sigma Aldrich), monoclonal anti-CD133-APC (eBiosciences), rat anti-BrdU (Santa Cruz Bio.), polyclonal anti-Nestin (Almqvist et al., 2002), monoclonal anti-Tuj1 (Covance), polyclonal anti-GFAP (Sigma Aldrich), monoclonal anti-Histone-3 (Abcam), polyclonal anti-phospho Rb (Cell Signaling), monoclonal anti-phospho p44/42 MAPK (Cell Signaling), monoclonal anti-p21, monoclonal anti-p27, anti-Myc, and anti-HA (Santa Cruz Bio). The secondary antibodies were anti-mouse IgG-HRP and anti-rabbit IgG-HRP (DAKO). Wortmannin (PI3 kinase blocker) and U0126 (MAP kinase blocker) were from Sigma Aldrich.

DNA constructs and transfection

Dominant negative cyclin D1 (T156A) was generously provided by Prof. Charles J. Sherr and constitutively active cyclin D1 (T286A) was procured from Addgene (Addgene plasmid 11182; submitted to Addgene by Dr. Bruce Zetter). Constitutively active forms of the PI3 kinase (pCG-p110*) and Erk kinase (pCEP-MEK*) were a kind gift from Dr. Jean-Francois Tanti. The reporter plasmids used here were 12XCSL-luciferase (Chapman et al., 2006) and the −1745 human cyclin D1 promoter luciferase reporter was kindly provided by Prof. Richard G. Pestell (Fu et al., 2005). The plox EGFP and pSalk-Cre were generously provided by Prof. George Daley. Transfections were carried out as described (Falk et al., 2007).

Immunocytochemistry

Immunoflourescence staining was done as described previously (Hansson et al., 2005). The immunoreactivity was visualized with Openlab software or Zeiss LSM510 META confocal unit. Images were cropped and assembled in Adobe Photoshop and arranged in Adobe Illustrator.

Western blot analysis

Western blots were produced as previously described (Laudon et al., 2005). The blots were then scanned and quantified with ImageJ software.

FACS analysis

Cells in cultures were washed with PBS, before trypsinizing and finally collected in ice-cold PBS supplemented with 4% FCS. These were then stained with fluorescent tagged antibodies against cell surface antigens, for 30 min on ice. The same was done with the isotype controls. The cells were then washed off the excess antibody using PBS with 4% FCS. For analysis of cells with nuclear cyclin D1, differential centrifugation was carried out to separate nuclear and cytoplasmic fractions. The nuclear fractions were then stained with cyclin D1 antibody prior to FACS analysis. The fluorescently stained cells were analyzed using FACS Aria.

Luciferase reporter assay

Transfections of the luciferase reporter constructs were carried out in 12-well tissue culture plates as have been described previously (Laudon et al., 2005). Where indicated, a pulse of doxycycline for 6 h was given to the cells 12 h post-transfection. Following this, cells were lysed with lysis buffer (10 mM Tris, pH8, 1 mM EDTA, 150 mM NaCl, and 0.65% Nonidet P-40) and monitored luminometrically for luciferase activity after adding luciferin (BioTherma) and ATP (BioTherma). The final luciferase values were normalized with reference to the β-galactosidase activity as an internal control. The values are represented as relative luciferase units.

Fig. 1. Generation and characterization of the Notch1ΔE^{TetOn} ES cell line. (A) Schematic representation of the generation of the Notch1ΔE^{TetOn} cell line from the starting AINV-15 vector (Kyba et al., 2002). Briefly, the AINV-15 vector contains the rtTA in the Rosa26 locus, and Notch1ΔE linked to EGFP was inserted by Cre recombination into the HPRT locus and placed under control of the tetracycline activation element. (B) Induction of Notch1ΔE production from the Notch1ΔE^{TetOn} cell line. Western blot of Notch1 ICD (recognized by an antibody specific for the new N-terminus in Notch1 ICD) demonstrates induction from 1 to 5 μg / ml doxycycline, and undetectable levels of Notch1 ICD in the absence of doxycycline. Loading control: reprobing with anti-β-actin (lower panel). (C) Loss of Notch1 ICD 12 h after removal of doxycycline. (D) Activation of 12XCSL-luc by 2 μg/ml doxycycline and blocking of activation by addition of DAPT in the presence of doxycycline. (E) Activation of the Notch downstream genes *Hey1* and *Hey2* by doxycycline (black bar), as compared to simultaneous addition of docxycycline and DAPT (grey bar) or uninduced cells (white bar). (F) Activation of EGFP expression by FACS. (G) Expression of pluripotency markers (Oct4, Sox 2, and SSEA1) along with DAPI in the Notch1ΔE^{TetOn} cells cultured in ES medium. Bar graphs (D, E) show average activity from triplicates of each experiment, error bars indicate standard deviation: ***Significant difference at $p<0.001$; **significant difference at $p<0.01$. Scale bar: 40 μm.

RNA preparation and quantitative RT-PCR

Total RNA extraction and quantitative PCR was performed as previously described (Sahlgren et al., 2008). The real-time quantitative PCR was conducted on ABI 7500 (Applied Biosystems) as suggested by the manufacturer. The primers were designed with PrimerExpress program from Applied Biosystems. Primers were used for (mouse) SOX1, Bcl 2, Cdc25A, E2F, Cyclin D1, Cyclin E, cMyc, Cyclin B1, Cyclin A,

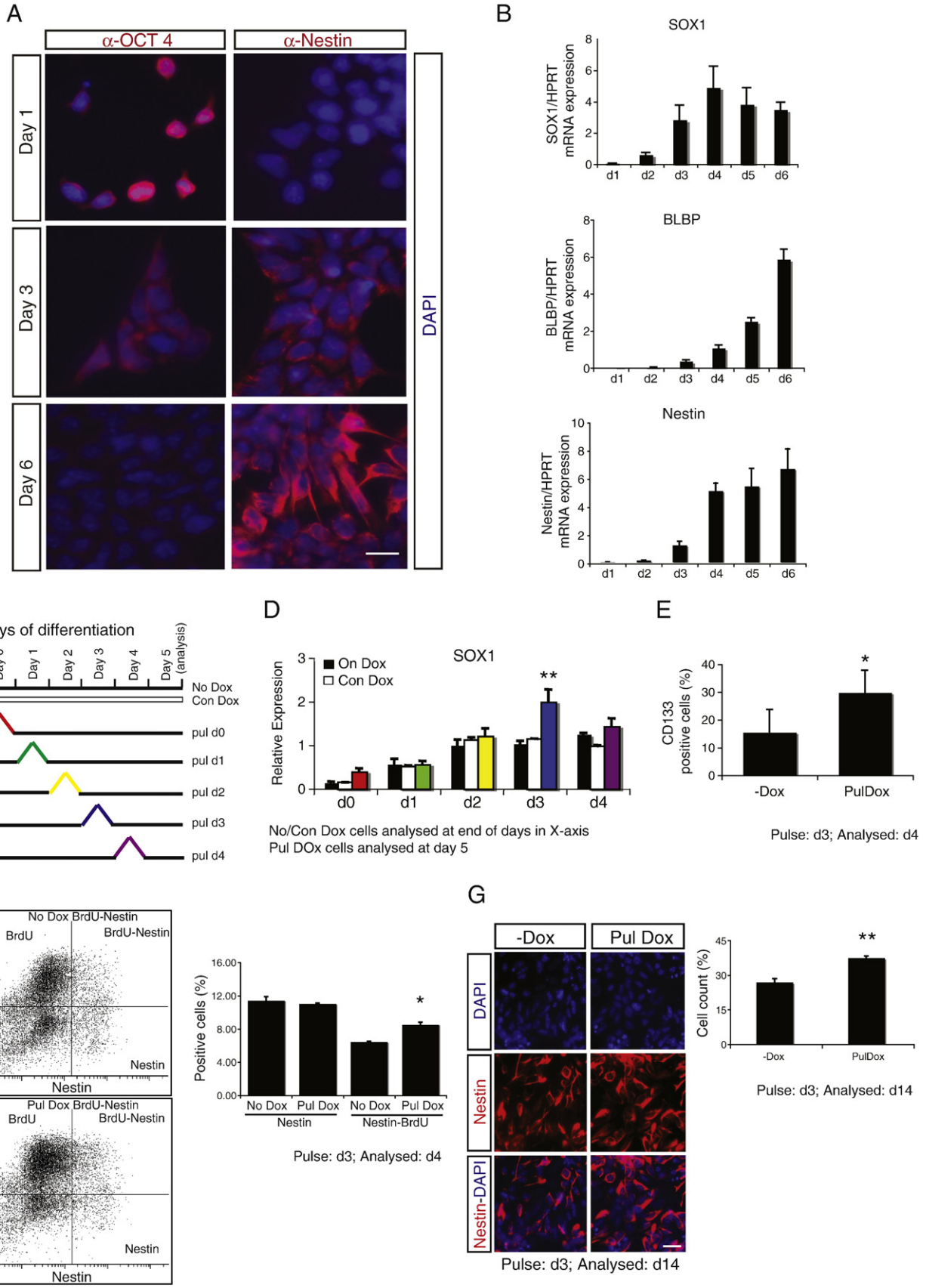

CDK4, CDK2, CDK1, GAPDH, and CDK6, and primer sequences are described in Supplementary Fig. 1.

Mouse ES cell culture and neural differentiation

The mouse ES cells were grown at a density of 3–6×10^5 cells/25 cm^2 under feeder free conditions, in ES medium containing DMEM (Invitrogen) supplemented with 10% knock-out serum (Invitrogen), 2% fetal calf serum, 0.1 mM nonessential amino acids, 1 mM sodium pyruvate (Invitrogen) and 0.1 mM 2-mercaptoethanol (Sigma). For neural differentiation, cells were grown in medium containing DMEM-F12 and Neurobasal medium (Invitrogen 1:1) with N2 supplement and B27 as additives. Briefly, 2×10^5 cells were plated on gelatinized 6-well plates for neural differentiation.

Embryonic neural stem cell cultures

Rat embryonic neural stem cells (NSCs) were derived as previously described (Gustafsson et al., 2005). Briefly, rat cortical tissue from embryonic day 15.5 was dissociated and 800×10^3 cells were plated per 10-cm dish that first had been coated with poly-L-ornithine and fibronectin (both from Sigma-Aldrich). NSCs were expanded in N2 media with 10 ng/ml of basic fibroblastic growth factor (R&D Systems) and subcultivated with mild dissociation in the presence of HBSS, NaHCO3, and HEPES (from Invitrogen and Sigma-Aldrich). Supplements were added daily, and medium was changed every second day. Animals were treated in accordance with national and institutional guidelines (Ethical permit no. N310/05).

Nucleofections

Nucleofections were performed according to the supplier's recommendations (Rat NSC kit, program A-33, AMAXA-Lonza). Three micrograms of plasmid cDNA and 3–4×10^6 cells were used for each nucleofection. Cells were plated in N2 medium supplemented with 10 ng/ml FGF-2. Treatment with 2.5 nM DAPT (Calbiochem #565770) was started the day after nucleofection. Cells were collected for qRT-PCR analysis 48 h after nucleofection.

Karyotype

ES cells were trypsinized and resuspended in single cell suspension in hypotonic solution (0.56% KCl). Cells were incubated in the hypotonic solution for 6 min before fixing in Carnoy's fixative (3:1; methanol:acetic acid). The chromosome spreads were prepared after washing in deionized water the preincubated slides in absolute ethanol and concentrated hydrochloric acid (1:1) the day before. The chromosomes were then stained with DAPI, visualized by using Zeiss Axiovert 200 M microscopy, and captured with digital camera.

Recombinant Jagged1 ligand-induced activation of endogenous Notch signaling

Endogenous Notch was activated using recombinant Jagged1 protein. Briefly, cell culture plates were coated on specific days initially with protein G, followed by recombinant human Fc (control) or Fc-Jagged1, as described in (Sahlgren et al., 2008). After washing off excess recombinant Jagged1, the plates were precoated with 0.1% gelatin prior to plating cells.

BrdU, propidium iodide staining, and caspase-3 staining

Cell proliferation was assayed using BrdU staining using APC BrdU Flow kit (BD Pharmingen) following the manufacturer's instructions. BrdU positivity was analyzed with FACSaria. Propidium iodide staining was conducted on ethanol-fixed cells resuspended in PI solution (10 ml 0.1% tritonX/PBS, with 2 mg DNase-free RNase A and 10 mg/ml propidium iodide solution). In order to study apoptosis, PE-conjugated polyclonal rabbit anti-active caspase-3 (BD pharmingen) was used. Cells were initially formalin fixed followed by permeabilization with Tween-20 and finally stained with the antibody, before analyzing with FACSaria. The cells with positive staining for activated caspase-3 were documented.

Mice

All histological analysis was carried out at the animal facility at the Department of Cell and Molecular Biology, Karolinska Institute, in accordance with the ethical regulations for mouse work in Sweden.

Results

Engineering a mouse ES cell line for temporally controlled activation of Notch

To be able to activate Notch with temporal precision in the ES cells, we engineered an ES cell line with inducible expression of an activated form of Notch, based on a previously described system for inducible gene expression (Kyba et al., 2002). We introduced a gain-of-function version of Notch1, Notch1 ΔE, linked to EGFP and tagged with myc into the pAINV-15 cells (Fig. 1A), and the resulting cell line is referred to as Notch1ΔE^{TetOn}. Notch1 ΔE was chosen as it represents a membrane-tethered, ligand-independent form of Notch, which upon cleavage by the γ-secretase complex generates a released Notch1 ICD that represents an activated form of Notch. An advantage of using the Notch1 ΔE form, in contrast to expressing only the Notch1 ICD, is that activity can be blocked by the use of γ-secretase inhibitors, and activity arising from expression from induction of Notch1 ΔE expression can thus be tested for being an authentic Notch response by pharmacological intervention by γ-secretase inhibitors.

We tested the efficacy of Notch1ΔE induction in the Notch1ΔE^{TetOn} cell line and the longevity of the produced protein, to determine the duration of pulsed Notch activation. There was no detectable production of Notch1 ICD (or Notch1 ΔE) in the absence of doxycycline, a tetracycline homologue, but at doxycycline concentrations ranging from 1 to 5 μg/ml, robust generation of Notch1 ICD was observed (Fig. 1B), although concentrations beyond 4 μg/ml seemed toxic (data not shown). Notch1 ICD levels were undetectable at 12 h after removal of doxycycline from the medium (Fig. 1C). This indicated that a good temporal control of Notch could be achieved in our Notch1ΔE^{TetOn} cell line. The rapid disappearance of Notch ICD after the withdrawal of doxycycline is most likely a consequence of

Fig. 2. Neural differentiation of the Notch1ΔE^{TetOn} cells after pulsed Notch activation. Immunocytochemistry for Oct4 and nestin in Notch1ΔE^{TetOn} cells at different stages of neural differentiation (days 1, 3, and 6) without doxycycline induction. (B) mRNA profiles for Sox1, BLBP, and nestin during neural induction in N2B27 medium. (C) Schematic representation of the scheme for pulsed activation of Notch during neural differentiation. A 6-h doxycycline pulse was given to the cells at day 0, 1, 2, 3, or 4 as indicated and cell analyzed at day 5 in neural differentiation. (D) Sox1 mRNA expression after no Notch activation, constant Notch activation, or a Notch pulse (for the pulse experiments, the color code indicates the day of doxycycline pulse as in panel C: red: pulse day 0, green: pulse day 1, yellow: pulse day 2, blue: pulse day 3, purple: pulse day 4, analysis at day 5). Constant Notch (white: constant doxycycline exposure for 4 days; analysis at the same day the cells are harvested). No Notch (black: no doxycycline stimulation; analysis at the same day the cells are harvested). (E) FACS analysis of CD133-positive cells on day 4 in neural induction after a day 3 pulse, as compared to untreated cells. (F) FACS plot showing Notch1ΔE^{TetOn} stained with BrdU and nestin after a pulse of Notch induction. The bar graph represents the quantification of the data in the FACS plot. (G) Immunocytochemistry (left) and FACS sorting (right) of nestin expression in Notch1ΔE^{TetOn} cells with/without pulse of doxycycline on day 3, analyzed on day 14 of neural differentiation. Bar graphs show average activity from triplicates of each experiment, error bars indicate standard deviation: **significant difference at $p<0.01$; *significant difference at $p<0.05$. Scale bars: A = 20 μm, G = 40 μm.

that an intracellularly "full-length" version of Notch1 ΔE was used, containing the C-terminal PEST domain, which is the target for ubiquitylation by cdc4 (Sel-10, Fbw7) followed by subsequent proteasomal degradation (Dohda et al., 2007; Oberg et al., 2001).

To learn whether the production of Notch1 ICD was accompanied by elevated Notch downstream signaling, we measured activation of the immediate downstream Notch reporter 12XCSL-luc. The 12XCSL-luc reporter activity was rapidly increased by doxycycline, and this increase was almost completely abrogated by the simultaneous addition of the γ-secretase inhibitor DAPT (Fig. 1D). In keeping with the elevated reporter activity, expression of the two Notch downstream genes *Hey1* and *Hey2* was observed (Fig. 1E). As an

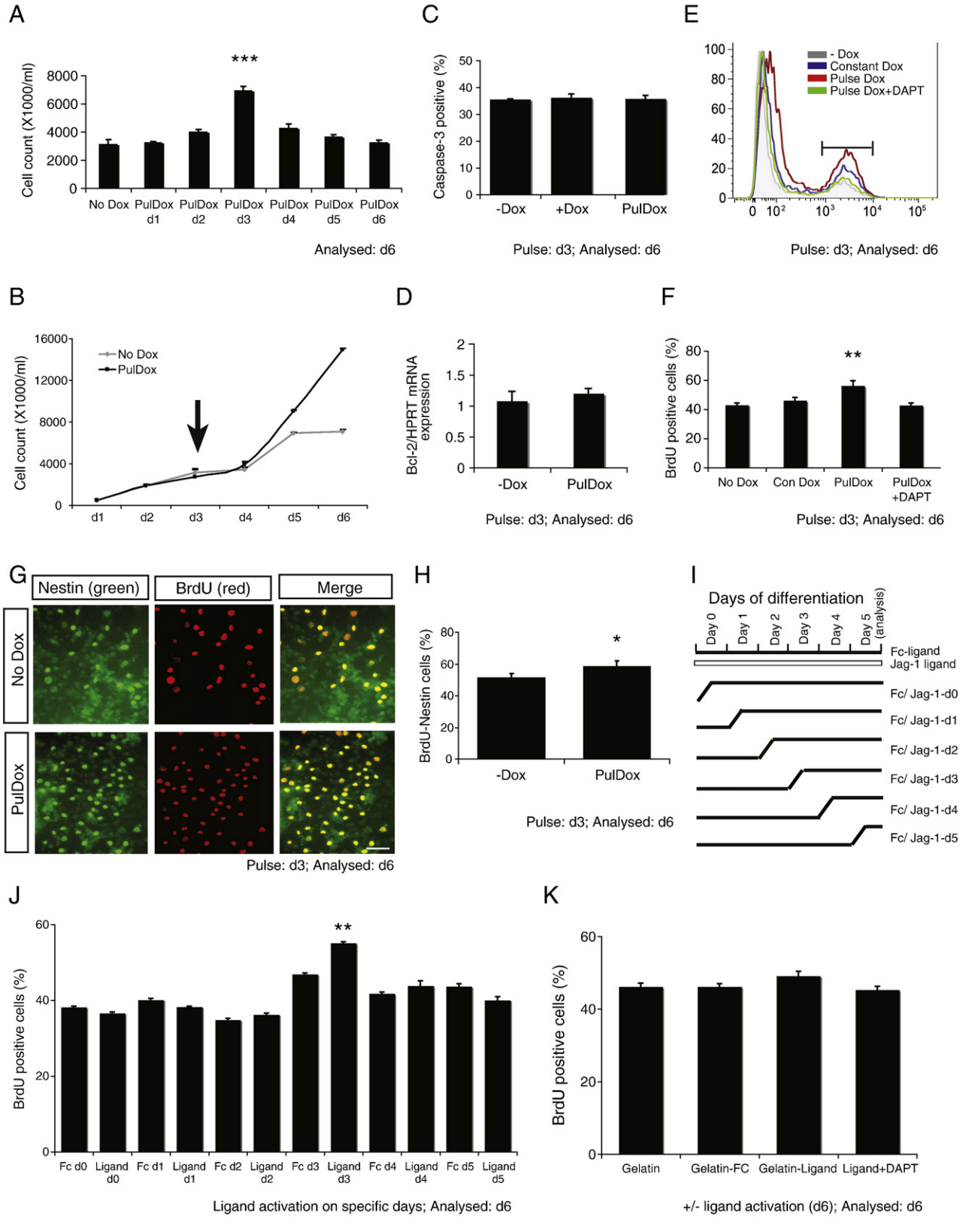

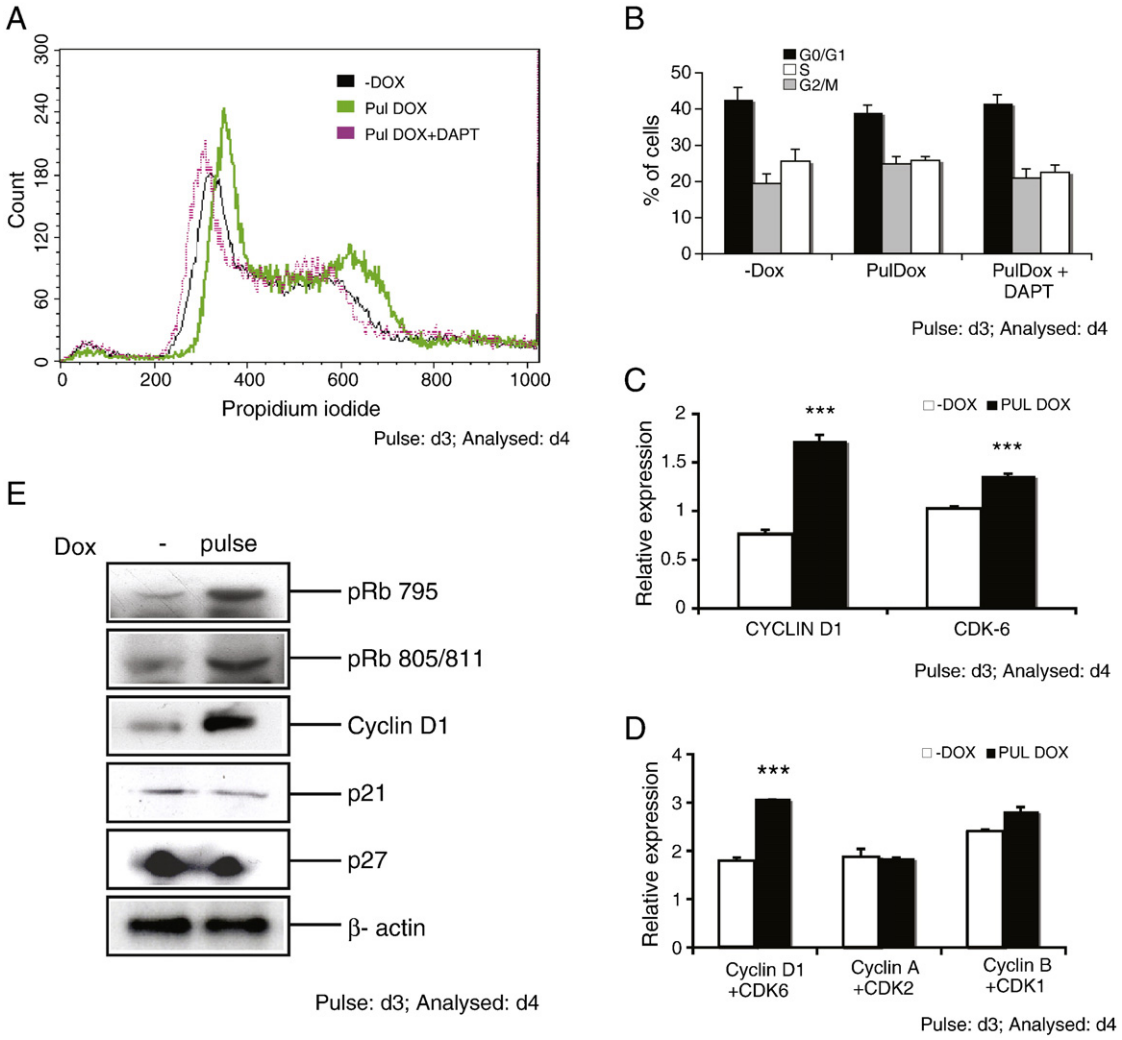

Fig. 4. Pulsed Notch signaling alters G1/S cell cycle control and activates cyclin D1. (A, B) Analysis of cell cycle distribution following a day 3 pulse, constant doxycycline or no doxycycline treatment. FACS plot (A) and the corresponding data in a bar graph (B). (C) Q-PCR analysis of cyclin D1 (left) and CDK6 (right) expression. (D) Q-PCR analysis of cyclin D1 + CDK6, cyclin A + CDK2, and cyclin B + CDK1 expression. (E) Western blot analysis of various cell cycle proteins, as indicated, in the absence of doxycycline (−) or after a 6-h pulse of doxycycline at day 3 (pulse). Analysis in panels A–E was performed at day 4 during neural differentiation, and the doxycycline pulse was given for 6 h on day 3, as indicated (pulse: d3). Bar graphs show average activity from triplicates of each experiment, error bars indicate standard deviation: ***significant difference at $p<0.001$.

independent confirmation of Notch activation in the Notch1ΔE^{TetOn} cells, we analyzed Notch induction by FACS, taking advantage of the EGFP fusion to Notch1 ΔE. Doxycycline stimulation for 6 h yielded approximately 70% EGFP-positive cells (Fig. 1F, Supplementary Fig. 2A), and no EGFP positive cells were detected in the unstimulated cells (Fig. 1F). To investigate whether the "negative" cell population, i.e., the 30% of cells with EGFP levels under the cutoff level in the FACS analysis, still expressed sufficient levels of Notch signaling for activation, we sorted out the negative population by FACS and showed that expression of Hey1 and Hey2 was upregulated (Supplementary Fig. 2B). Moreover, mRNA expression of Notch1 ICD linked with GFP could be confirmed by Q-PCR in the sorted "negative" population (data not shown). This is in keeping with previous observations that only very small amounts of Notch ICD are required to effectuate signaling (Karlstrom et al., 2002). Finally, we confirmed that the Notch1ΔE^{TetOn} cells expressed the ES stem cell markers Oct4, Sox2, and SSEA-1, when cultured in the ES medium at the undifferentiated state (Fig. 1G), and approximately 74% of the cells were karyotypically normal (Supplementary Fig. 2C).

Activation of Notch at day 3 leads to increased Sox1 and CD133 mRNA expression

A protocol for robust induction of early neural differentiation in ES cells has been developed, where ES cells are shifted from ES medium containing LIF (Leukemia Inhibiting Factor) to N2B27 medium

Fig. 3. A pulse of Notch signaling at day 3 results in increased proliferation. (A) Analysis of cell number after pulsed Notch activation at day 1, 2, 3, 4, 5, or 6 during neural induction. (B) Total cell number in cells pulsed at day 3 (arrow) or not treated with doxycycline for days 1–6 of neural induction. (C) Analysis of activated caspase-3-positive cells after a day 3 pulse, constant doxycycline treatment or in untreated cells. (D) Bcl-2-specific mRNA expression profile after a day 3 pulse, as compared to untreated cells. Analysis was performed at day 6 during neural differentiation. (E, F) Proportion of BrdU-positive cells after a day 3 pulse, constant doxycycline treatment or in untreated cells, or after a combination of a day 3 doxycycline pulse and DAPT. The FACS plot is shown in panel E and the corresponding data in a bar graph in panel F. (G, H) Proportion of cells co-expressing nestin and BrdU after a day 3 pulse as compared to untreated cells. Immunocytochemistry (G) and the data in a bar graph (H). (I) Schematic representation of the scheme for induction of endogenous Notch signaling. (J) Bar graph showing the BrdU-positive population detected after plating the Notch1ΔE^{TetOn} cells on immobilized ligand, as described in panel I. Samples were analyzed on day 6 of neural differentiation. (K) BrdU-positive population of Notch1ΔE^{TetOn} cells that had been cultured on Jagged1 or Fc ligand as indicated for 6 days during neural differentiation. Analysis in panels A–K was performed at day 6 of neural differentiation. Bar graphs show average activity from triplicates of each experiment, error bars indicate standard deviation: ***significant difference at $p<0.001$; **significant difference at $p<0.01$; *significant difference at $p<0.05$. Scale bar: 40 μm.

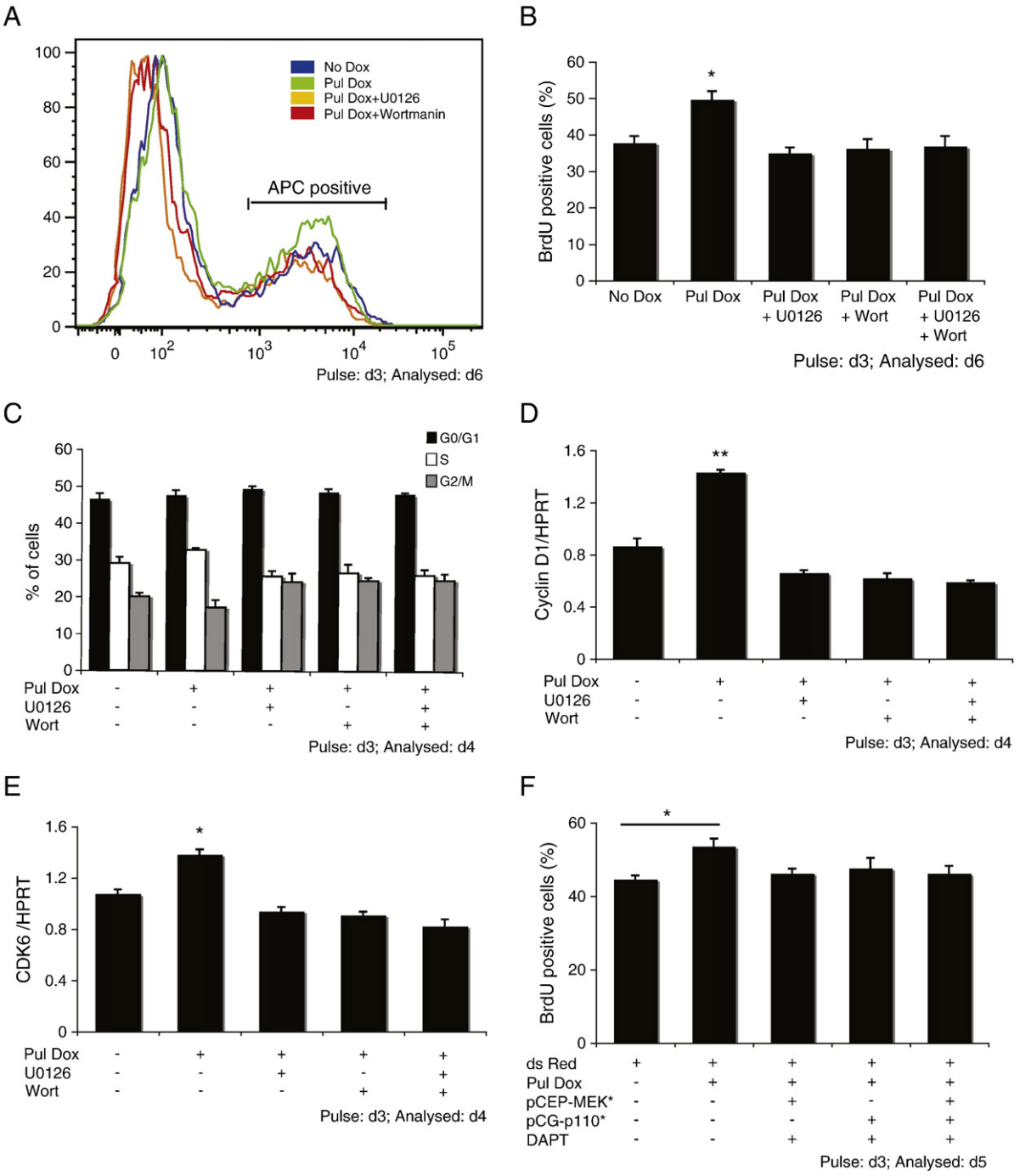

Fig. 5. Blocking of PI3 kinase and MAP kinase abrogates Notch-induced proliferation and cyclin D1 and CDK6 expression. (A, B) Analysis of the BrdU-positive cell population in the absence and presence of doxycycline pulse and with pharmacological inhibition of MAP kinase (U0126) and PI3 kinase signaling (Wortmannin). Wortmannin and U0126 were added 30 min prior to Notch activation. The histogram (A) depicts the BrdU–APC population, and the bar graph (B) depicts the percentage of BrdU-positive cells. (C) Analysis of cell cycle stages in the presence of U0126 and Wortmannin alone or in combination. (D, E) Quantitative PCR analysis of cyclin D1 (D) and CDK6 (E) mRNA levels after Notch activation in the presence or absence of U0126 and Wortmanin alone or in combination, as indicated. (F) Notch1ΔE^{TetOn} cells were transfected with dsRed alone or in combination with pCEP-MEK* or pCG-p110* to activate MAP and PI3 kinase signaling, respectively. Notch signaling was then blocked with DAPT. The bar graph depicts BrdU labeling in cells with activated or blocked Notch signaling in various combinations with activated Erk or PI3 kinase signaling, as indicated. Bar graphs show average activity from triplicates of each experiment, error bars indicate standard deviation: ***significant difference at $p<0.001$; **significant difference at $p<0.01$; *significant difference at $p<0.05$.

supplemented by β-mercaptoethanol, and cultured for 6 days in monolayer culture (Stavridis and Smith, 2003). The Notch1ΔE^{TetOn} cells did undergo the expected differentiation when subjected to this protocol, i.e., a progressive loss of Oct4 and a gain in nestin protein expression was observed (Fig. 2A). At the mRNA level, an increase in expression of Sox1, BLBP, and nestin was noted during neural differentiation (Fig. 2B).

To explore temporal context dependency for Notch, we set up a scheme where a 6 h doxycycline pulse was given at day 1, 2, 3, 4, or 5 during the early neural differentiation, and the effects were analyzed at day 6 (schematically summarized in Fig. 2C). In a parallel set of experiments, the effects of constant exposure to doxycycline were tested, and here cells were harvested and directly analyzed at each day (0–4) during neural induction. As Sox1 is an early neural progenitor marker, and upregulated in the earliest phase of neural induction (Lowell et al., 2006), we deployed this inductive scheme to learn whether Sox1 expression was altered upon temporal activation

of Notch. The results revealed a significant increase in the transcription of Sox1 in cells pulsed with doxycycline on day 3, in comparison to cells pulsed at other days, constantly exposed or not exposed at all to doxycycline (Fig. 2D). Similarly, expression of CD133 (prominin 1), which is expressed in neural progenitors (Peh et al., 2009), was elevated by a day 3 pulse of Notch signaling, when analyzed on day 4 (Fig. 2E). The increase appeared to be transient, as analysis at a later timepoint, day 9 during neural differentiation, did not yield a significant difference in expression of CD133 (data not shown). Along with the increased amount of CD133 mRNA, an increase in the Nestin–BrdU double-positive population was observed at day 4, although the total number of nestin-positive cells did not increase at day 4 (Fig. 2F). Upregulation of the proportion of nestin-expressing cells was, however, observed when analyzed 14 days after neural induction, following a day 3 pulse (Fig. 2G). Given the observed increase in the Sox1 mRNA and CD133 protein levels, we were interested if there were also effects on the choice between commitments to the glial versus neuronal lineages, following a longer period of differentiation. To address this, we cultured the Notch1ΔE^{TetOn} cells as monolayer in neural differentiation medium with or without a short pulse of doxycycline at day 3 for 6 additional days. Analysis of Tuj1 (β-III-tubulin) and GFAP expression, as markers for early neurons and astrocytes, respectively, revealed no significant difference in the proportion of Tuj1- or GFAP-expressing cells between the cultures exposed to a day 3 pulse of doxycycline versus no doxycycline stimulation (Supplementary Fig. 3).

Activation of Notch at day 3 leads to increased proliferation

The elevation in Sox1 and CD133 expression specifically following a day 3 doxycycline pulse spurred us to investigate whether pulsed activation at day 3 may also affect cell number. A 6 h doxycycline pulse was given to the cells at day 1, 2, 3, 4, or 5 and the total number of cells was analyzed at day 6. The results showed that pulsing the cells at day 3 led to a significant upregulation in the number of cells at day 6, as compared to pulsing the cells at the other days (Fig. 3A). We next made a time course of the increase in cell number by analyzing the total number of cells at each day during the 6 day neural induction in two parallel cell cultures: one cultured in the absence of doxycycline and the other pulsed for 6 h at day 3. There were, as expected, no significant difference in cell number at days 1–3 (i.e., before or at the doxycycline pulse), but starting at day 4, we noted a small increase in cell number in the day-3-pulsed cells, which was further augmented at days 5 and 6 (Fig. 3B).

The increase in cell number could be a result of a decrease in apoptosis and/or an increase in the proliferative rate. We first analyzed apoptosis by staining for activated caspase-3, but no increase in the proportion of cells expressing activated caspase-3 after the day 3 pulse, or after constant doxycycline stimulation, was observed (Fig. 3C). Staurosporine-exposed cells were used as positive control for measuring activated caspase-3 (data not shown). Moreover, the expression of Bcl-2, an anti-apoptotic marker, was not significantly altered by the day 3 pulse (Fig. 3D). To study a possible change in proliferation, we analyzed the incorporation of BrdU under the different conditions. Cells subjected to constant doxycycline stimulation, a day 3 pulse, or left untreated were supplemented with BrdU in the culturing medium for 1 h at day 6, and the proportion of BrdU-expressing cells was analyzed 1 h after the BrdU administration. In the untreated cells and in the cells with constant doxycycline induction, there were 43% and 46% BrdU-positive cells, respectively, and this was significantly increased in the day 3 pulse cells (56%) (Fig. 3E, F). Blocking Notch signaling by DAPT in the day 3 pulse cells abrogated the increase in the number of BrdU-positive cells, bringing it back to 42% (Fig. 3F). To learn whether the increase in the proportion of BrdU$^+$ cells was confined to a particular cell population, we determined the proportion of cells that were double-positive for BrdU and nestin, GFAP or Tuj1. The proportion of BrdU$^+$/nestin$^+$ cells was significantly increased in the day-3-pulsed cells (Fig. 3G, H). In contrast, no significant difference was observed for the BrdU$^+$/GFAP$^+$ cells or BrdU$^+$/Tuj1$^+$ cells (Supplementary Fig. 4). To corroborate the finding that Notch induction by doxycycline stimulation enhanced proliferation, we tested whether activation of Notch signaling through endogenous Notch receptors yielded a similar result. Endogenous Notch signaling was activated by plating Notch1ΔE^{TetOn} cells that were not doxycycline stimulated on immobilized recombinant Jagged1 ligand on specific days during neural differentiation until the day of analysis, to mimic as closely as possible the transient induction by a doxycycline pulse (Fig. 3I). Ligand activation was confirmed by activation of Hey1 mRNA expression (Supplementary Fig. 5), and ligand stimulation at day 3 during neural induction, but not at the other days, led to an increase in the proportion of BrdU-positive cells, as compared to cells cultured on only Fc fragment as control (Fig. 3J). When the Notch1ΔE^{TetOn} cells were grown for 48 h on Jagged1, mimicking constant Notch stimulation, no effect on proliferation was observed (Fig. 3K). These data suggest that activation of Notch signaling specifically at day 3 enhances cellular proliferation.

Pulsed Notch activation at day 3 alters G1/S cell cycle control and activates cyclin D1

The Notch-mediated increase in cell number and proliferation may be related to changes in cell cycle control. To explore in which phase of the cell cycle Notch exerted its effect, day-3-pulsed or untreated cells were labeled with propidium iodide and analyzed by FACS for cell cycle phase distribution. The data revealed a slight increase in the number of day-3-pulsed cells in S phase and a corresponding slight decrease in the G0/G1 stage (Fig. 4A, B). This shift in the balance of S phase versus G0/G1 phase was abrogated by the addition of DAPT (Fig. 4A, B).

This indicated a modulation at the G1/S transition check point and to explore how Notch impinges on the G1/S control, we searched for changes in the expression of genes controlling various phases of the cell cycle. Cyclins and Cyclin-dependent kinases (CDKs) are key cell cycle regulators: cyclin D1 and CDK6 control the G1/S, cyclin A and CDK2 control the G2 phase, whereas cyclin B and CDK1 control the M phase check point. Analysis of mRNA expression levels revealed no significant changes for cyclin E, cyclin B1, cyclin A, CDK1, CDK2, and CDK4 mRNAs (Supplementary Fig. 6), whereas, in contrast, cyclin D1 and CDK6 mRNAs were significantly upregulated by the day 3 pulse, as compared to untreated cells, when analyzed at 12 h post doxycycline induction (Fig. 4C). Furthermore, when the combined expression of cyclin D1 and CDK6 mRNAs was compared to the combined expression of cyclin A and CDK2 or cyclin B and CDK1 in day-3-pulsed and untreated cells, a significant upregulation was observed only for the cyclin D1 and CDK6 combination (Fig. 4D). In keeping with the elevated mRNA expression, cyclin D1 was also upregulated at the protein level (Fig. 4E). The altered G1/S transition following a day 3 pulse was manifested also by an increase in phosphorylated forms of the retinoblastoma protein (pRb 795 and pRb 805/811) and a decrease in the cell cycle blockers p21 and p27 (Fig. 4E). The data suggested that the proliferative increase occurred during the induction phase of neural differentiation, corresponding to day 3, rather than at a more mature neural stem cell state, corresponding to day 6. To explore the Notch–cyclin D1 relationship in primary neural stem cells, we analyzed the effect of Notch activation in cortical progenitor cells derived from embryonic day (E) 15 rat embryos. The level of cyclin D1 mRNA expression was increased after transfection of Notch1 ICD, and as expected, this increase was not abrogated by DAPT (Supplementary Fig. 7A). As a control, the level of Hes5 mRNA expression was also increased by Notch1 ICD transfection (Supplementary Fig. 7B), and as expected

since Notch1 ICD was used, the upregulation could not be blocked by addition of DAPT (Supplementary Figs. 7A,B). In conclusion, these data point to an effect on the G1/S transition by Notch activation at day 3 during neural differentiation, linked with increased expression of cyclin D1, and an ensuing increase of phosphorylated Rb protein.

The Notch-mediated proliferative effect requires functional PI3 and MAP kinase signaling

As Notch signaling extensively cross-talks with other signaling pathways (for review, see Hurlbut et al., 2007; Lendahl et al., 2009;

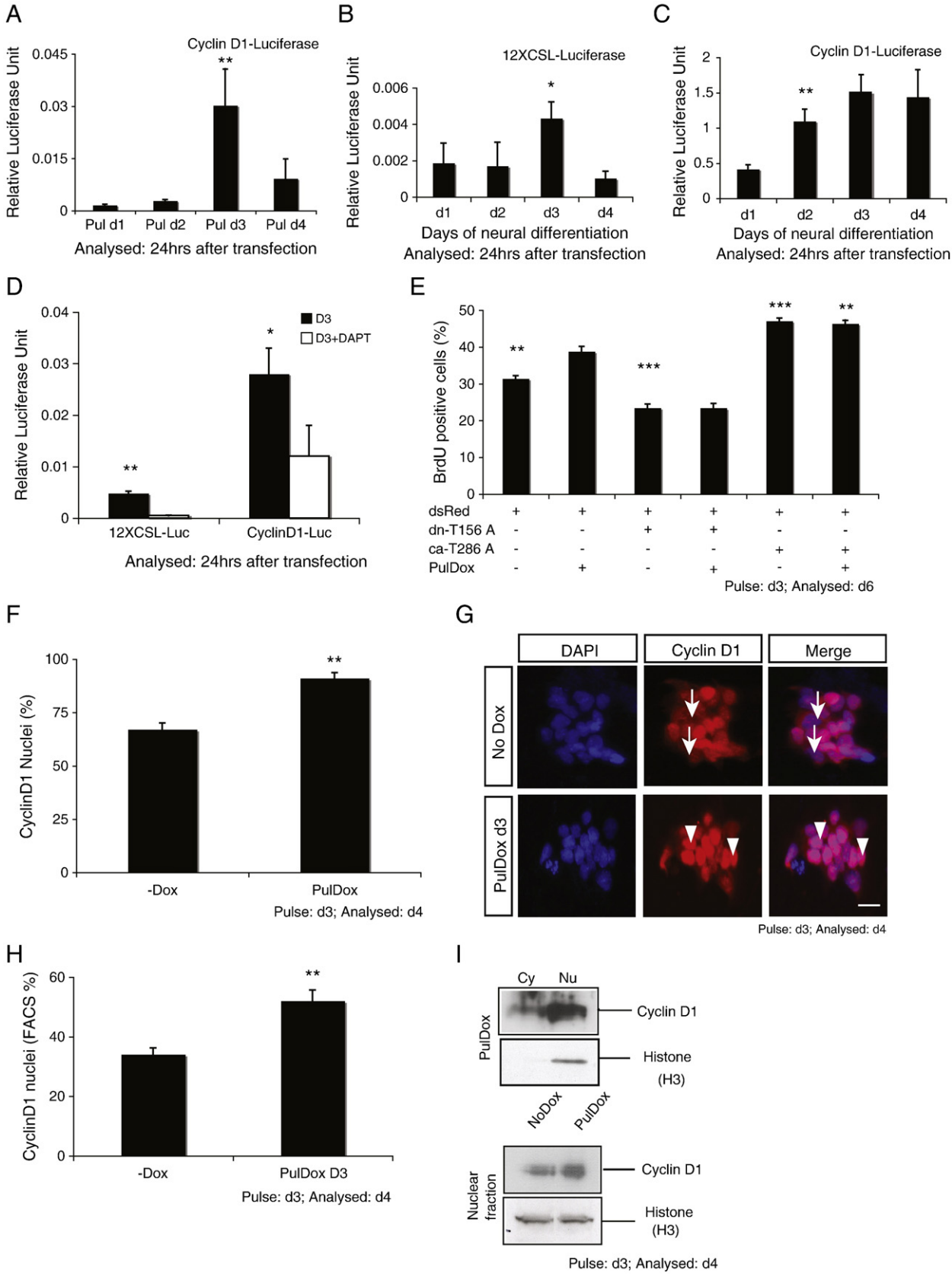

Poellinger and Lendahl, 2008), we wanted to learn whether the increase in proliferation and gene expression by the day 3 pulse required the activity of other signaling pathways. Blocking of the MAP kinase pathway by the inhibitor Erk kinase inhibitor U0126 or blocking PI3 kinase signaling by the inhibitor Wortmannin resulted in an abrogation of the increase in the proportion of BrdU-positive cells observed after the doxycycline pulse at day 3 (Fig. 5A, B). The increase in the proportion of cells in S-phase, at the expense of cells in G2/M phase, observed after Notch induction, was abrogated by treatment with U0126 or Wortmannin alone or in combination, and blocking MAP or PI3 kinase signaling in fact led to a further increase in G2/M phase and a corresponding reduction of the number of cells in S phase (Fig. 5C, Supplementary Fig. 8A). The elevation of cyclin D1 and CDK6 mRNA levels observed after Notch induction at day 3 were abrogated by U0126 and Wortmannin treatment alone or in combination (Fig. 5D, E). Finally, to address if activated MAP or PI3 kinase signaling could substitute for activated Notch signaling in the induction of proliferation, we treated the Notch1ΔE^{TetOn} cells with DAPT to block Notch signaling and then activated Erk and PI3 kinase signaling by transfecting pCEP-MEK* and pCG-p110*, which represent constitutively active forms of Erk and PI3 kinase, respectively, along with dsRED plasmid. DsRED-expressing cells were then sorted and analyzed for BrdU incorporation. Expression of the constitutively active forms of Erk and PI3 kinase (for control of expression levels of pCEP-MEK* and pCG-p110*, and activity of pCEP-MEK*, see Supplementary Fig. 8B, C) was not sufficient to induce the increase in BrdU-positive cells observed after Notch activation by doxycycline at day 3 (Fig. 5F). In sum, these data indicate that the Notch-mediated proliferative effect requires MAP and PI3 kinase signaling but that activated MAP and PI3 kinase signaling cannot induce this effect in the absence of Notch signaling.

Cyclin D1 is critically required for the Notch-mediated effect on proliferation

To study whether the activation of cyclin D1 by Notch in the ES cells involved regulation at the transcriptional level, we tested whether a 1.7-kb cyclin D1 promoter element was responsive to pulsed Notch activation during early neural induction. When the Notch1ΔE^{TetOn} cells were given a 6-h doxycycline pulse at day 1, 2, 3, 4, or 5, we observed that the cyclin D1 promoter-luciferase reporter construct (Leslie et al., 2006) was significantly upregulated only by a pulse at day 3 (Fig. 6A). The enhanced activation of the cyclin D1 promoter at day 3 led us to analyze whether day 3 represented a unique stage also with regard to endogenous Notch activation and cyclin D1 expression. We tested this by transfecting in the Notch reporter construct 12XCSL-luc or a cyclin D1-luciferase reporter construct at different days of neural differentiation and then recorded the reporter gene activity in untreated cells, i.e., under endogenous Notch signaling conditions, at 24 h post-transfection. In both cases, there was an increase in reporter gene activity up to days 3 and 4 (Fig. 6B, C, Supplementary Fig. 9). Both the Notch-induced cyclin D1-luc and 12XCSL-luc activation could be blocked by DAPT (Fig. 6D). Together, these data suggest that there is a peak of endogenous Notch activity at day 3, a stage which also exhibits enhanced cyclin D1 promoter activity.

The effect on cell proliferation and the direct upregulation of cyclin D1 by doxycycline stimulation suggests, but does not directly prove, that cyclin D1 is the "culprit" of Notch activation resulting in increased cell proliferation. To address this issue, we tested whether expression of a dominant-negative version of cyclin D1 (cyclin D1-T156A) could override the Notch-induced cell proliferation. When Notch1ΔE^{TetOn} cells were transfected with the cyclin D1-T156A construct at day 2 (and co-transfected with dsRED to allow for FACS sorting for expressing cells followed by a doxycycline pulse at day 3, and analysis at day 6), we noted a significant reduction in the proportion of BrdU-positive cells, as compared to cells that were pulsed and only dsRED-transfected and FACS sorted (Fig. 6E). The percentage of BrdU-positive cells was reduced by cyclin DN-T156A to a level below the dsRED-only-transfected cells (Fig. 6E; for transfection efficiency, see Supplementary Fig. 10), suggesting that endogenous cyclin D1 function was also reduced, resulting in a further reduction in cell proliferation. Conversely, transfection of a constitutively active form of cyclin D1, cyclinD1-T286A, increased cell proliferation to a similar extent both in the untreated and in the day-3-pulsed cells (Fig. 6E, for transfection efficiency see Supplementary Fig. 10), indicating that elevated expression of cyclin D1 can substitute for Notch activation.

Cyclin D1 can be localized both to the nucleus and the cytoplasm, and an altered nuclear versus cytoplasmic ratio has been reported in response to different stimuli (Alt et al., 2000). We were therefore curious to learn whether the upregulation of cyclin D1 expression by the brief activation of Notch at day 3 affected the intracellular distribution of cyclin D1. Cells subjected to a 6-h doxycycline pulse showed a more prominent nuclear distribution, as compared to non-induced cells, i.e., 91% of the day-3-pulsed cells exhibited a nuclear expression, versus 67% of the non-induced cells (Fig. 6F, G). FACS analysis of cyclin-D1-positive cell nuclei revealed a similar increase in the proportion of cyclin-D1-positive nuclei: 50% versus 38% for pulsed and non-induced cells, respectively (Fig. 6H). The increase in nuclear localization of cyclin D1 observed in Fig. 6F–H was paralleled with an increase in the amount of cyclin D1 in the nucleus after the day 3 doxycycline pulse, as judged by Western blot analysis (Fig. 6I). In conclusion, these data reveal that Notch controls cyclin D1 expression and that cyclin D1 is a critical mediator of the Notch-induced effect on proliferation.

Reduced cyclin D1 expression in mice with defective Notch signaling

To address whether the level of cyclin D1 expression was controlled by Notch expression also in the developing CNS in vivo, we compared the distribution of cyclin D1 in the developing spinal cord of E10.5 wild-type and Jagged$^{Ndr/Ndr}$ mouse embryos (Fig. 7A–F). Jagged$^{Ndr/Ndr}$ mice carry a missense mutation in the Jagged1 ligand, which renders the Jagged1 ligand signaling incompetent (Hansson et al., 2010). Cyclin D1 expression was predominantly confined to a specific dorsoventral domain, the dp6 domain, and with considerably lower expression in the flanking p0 and p2 domains in the E10.5 embryo (Fig. 7B, C). The dp6 domain also exhibited high levels of

Fig. 6. Cyclin D1 is required for the Notch-mediated effect on proliferation. Activation of a cyclin D1-luciferase reporter construct after pulsed activation of Notch at day 1, 2, 3, or 4, as indicated. (B) Activation of the 12XCSL-luciferase reporter under endogenous Notch conditions. (C) Analysis of cyclin D1-luciferase reporter under endogenous Notch conditions. Analysis in panels A–C was carried out 24 h post-transfection. (D) Activation levels of 12XCSL-luciferase and cyclin D1-luciferase reporters in response to DAPT treatment. (E) Analysis of the effects of dominant negative (dn-T156A) or constitutively active (caT286A) cyclin D1 forms on the Notch-induced increase in proliferation. The dsRED plasmid was transfected alone (two leftmost lanes) or in combination with dn-T156A/caT286A to allow for FACS sorting of transfected cells. The samples were analyzed on day 6. The statistical significance was calculated with respect to the BrdU positive population in PulDox cells. (F) The proportion of cells with nuclear cyclin D1 in control (−Dox) and day-3-pulsed (PulDox) cells. Analysis was performed on day 4 during neural induction, and cells positive for cyclin D1 were counted under the microscope. (G) Immunocytochemistry of intracellular localization of cyclin D1 in response to pulsed Notch activation and analyzed on day 3 post activation of Notch signaling. Arrows denote DAPI-stained cell nuclei not expressing cyclin D1, whereas arrowheads denote DAPI-stained nuclei expressing cyclin D1. (H) Proportion of cyclin D1-positive cell nuclei in control (−Dox) and day-3-pulsed (PulDox) cells as analyzed on day 4 during neural induction. (I) Western blot analysis of cyclin D1 content in the cytoplasmic (Cy) and nuclear (Nu) fractions. Reprobing with Histone 3 antibody as control for nuclear fractionation. Below, comparison of the amount of nuclear cyclin D1 in uninduced and day-3-pulsed cells. Reprobing with Histone 3 antibody as internal control. Analysis was carried out at day 4 during neural induction. Bar graphs show average activity from triplicates of each experiment, error bars indicate standard deviation: ***significant difference at $p<0.001$; **significant difference at $p<0.01$; *significant difference at $p<0.05$. Scale bar = 20 μm.

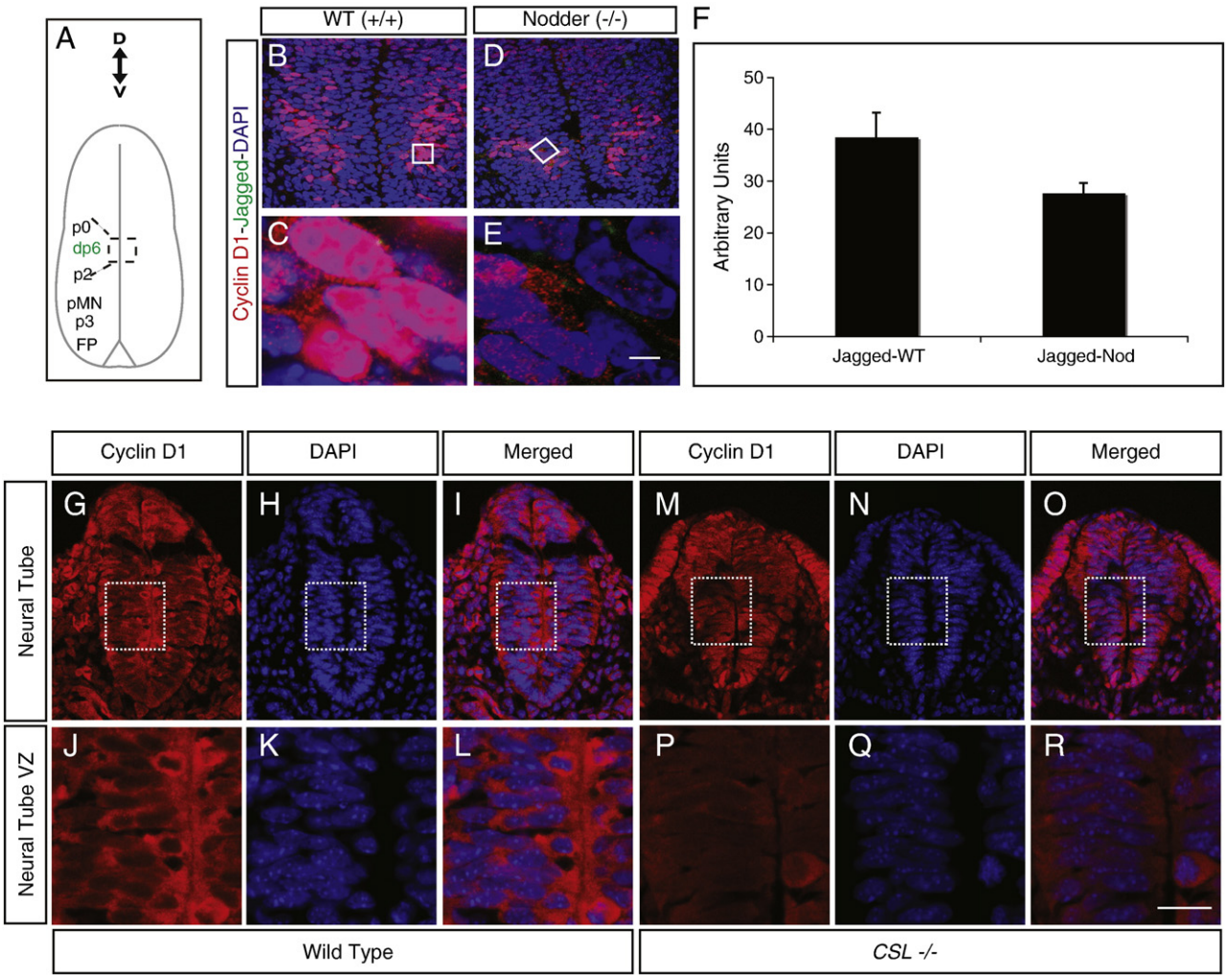

Fig. 7. Absence of Notch signaling decreases expression of cyclin D1. (A) Schematic representation of the embryonic spinal cord, where the area shown in panels B and D is indicated (rectangle). The various dorsoventral progenitor domains at the ventral side of the spinal cord are denoted (FP = floor plate) and the dp6 domain expresses Jagged1 (data not shown and Lindsell et al., 1996; Mitsiadis et al., 1997). Panel B represents a section from an E10.5 wild-type embryo (10× magnification in panel C), whereas panel D represents a section from a (Jagged1$^{Ndr/Ndr}$ (Nodder)) littermate embryo (10× magnification in panel E). The sections are stained for cyclin D1 (red) and DAPI (blue). (F) Average of the quantified results for nuclear cyclin D1 expression in both wild-type and Jagged1$^{Ndr/Ndr}$ littermate mouse embryos derived from three different litters. (G–H) Neural tube section of E8.5 wild-type and CSL$^{-/-}$ mice. Sections stained with cyclin D1 (red) and DAPI (blue). Scale bars: (B, D = 50 μm; C, E = 5 μm; G, H, I, M, N, O = 50 μm; J, K, L, P, Q, R = 20 μm.

Jagged1 expression (data not shown), in keeping with previous studies (Lindsell et al., 1996; Marklund et al., 2010). A reduced level of cyclin D1 expression in the Jagged$^{Ndr/Ndr}$ embryo was observed (Fig. 7D, E), as compared to the wild-type littermate embryo (Fig. 7B, C). Furthermore, the proportion of cells with nuclear cyclin D1 expression was higher in the wild-type mice (Fig. 7C), as compared with the Jagged$^{Ndr/Ndr}$ embryos (Fig. 7E; quantified in Fig. 7F). To corroborate the findings from the Jagged$^{Ndr/Ndr}$ embryos, we analyzed cyclin D1 distribution in mice deficient for CSL. CSL$^{-/-}$ E8.5 mouse embryos showed a significantly reduced cyclin D1 immunostaining in the corresponding region of the developing neural tube (Fig. 7G–R).

Discussion

Signaling mechanisms controlling cell fate decisions at multiple stages in a cell lineage must be able to interpret a temporally changing cellular context and integrate this information to generate a signaling output appropriate for each particular temporal stage in the cell lineage. In this report, we provide evidence that activation of the Notch pathway at different stages of early neural differentiation in mouse ES cells produces a stage-specific output: a brief activation at day 3 during neural differentiation leads to an increase in cell number and elevated expression of cyclin D1, and cyclin D1 is critically required for the observed increase in cell number.

The increase in cell number following a day 3 pulse is likely caused by enhanced proliferation, as BrdU incorporation was elevated, but without a significant reduction in apoptosis. The increase in cell number was accompanied by a shift in cell cycle phase distribution, with a small increase in the proportion of cells in S phase and a corresponding decrease of the number of cells in the G1 phase. Analysis of the key cell cycle components revealed a promotion of the G1/S transition, as the levels of cyclin D1 and CDK6, but not of other cyclins or CDK proteins, were elevated. The fact that the level of cyclin D1 mRNA was upregulated, and that a 1.7-kb cyclin D1 promoter was responsive to activation of Notch, suggests that cyclin D1 is a direct Notch target gene in mouse ES cells. The Notch-mediated increase in cellular proliferation and cyclin D1 and CDK6 expression required functional MAP and PI3 kinase signaling, as pharmacological intervention with these two pathways abrogated the Notch-mediated effect. Notch activation was, however, required, as no increase in proliferation or cyclin D1 and CDK6 expression was observed when MAP and PI3 kinase signaling was activated under conditions of blocked Notch signaling.

Our data indicate that the Notch-induced increase in cyclin D1 levels is critical for the observed increase in cell proliferation. Firstly,

the enhanced level of cyclin D1 was accompanied by elevated phosphorylation of the Rb protein and decreased levels of the two cell cycle inhibitors p21 and p27. Secondly, expression of a dominant negative cyclin D1 abrogated the increase in proliferation observed after Notch activation at day 3. Thirdly, expression of a constitutively active form of cyclin D1 was, in the absence of Notch activation, sufficient to mediate a proliferative effect similar to that observed after the brief Notch activation. Collectively, this argues that the Notch-mediated effect proceeds through activation of cyclin D1. The notion that Notch regulates cyclin D1 expression in early neural differentiation receives support also by the observation that cyclin D1 immunoreactivity was reduced in areas of active Notch signaling in the developing CNS in two mouse models deficient for functional Notch signaling. The finding that cyclin D1 is a downstream target gene of Notch is in keeping with previous observations from other cell types, such as tumor cells (Ronchini and Capobianco, 2001) and cardiomyocytes (Campa et al., 2008). The identification of cyclin D1 as the critical Notch downstream mediator of proliferation furthermore extends a recent finding on expression of cyclin D1 in early cortical differentiation in the mouse, where elevated cyclin D1 levels promoted generation and expansion of the CNS progenitor cell pool (Lange et al., 2009).

The data presented here not only provide evidence for a Notch-induced increase in cyclin D1 expression and cell proliferation but also identify day 3 in neural differentiation of ES cells as a temporal state endowed with special properties. In addition to the specific Notch response, day 3 is also characterized by a strong increase in Sox1 expression, and upregulation of the neural markers nestin and BLBP. We, however, cannot yet tell whether the specific upregulation of cyclin D1 by Notch at day 3 is a consequence of Notch signaling becoming more effective, upregulating a broader repertoire of genes, or whether the cyclin D1 gene specifically becomes more susceptible to upregulation. The fact that the 12XCSL-reporter activation was elevated at day 3 also under endogenous Notch signaling conditions may support the notion that this stage is generally more sensitized to Notch signaling, but to understand this will require further analysis of the global Notch signaling output and the chromatin state of the cyclin D1 promoter.

We found that Notch enhanced the proportion of neural progenitors, defined by expression of nestin, BLBP and CD133, but did not significantly affect the ratio between GFAP- and β-III-tubulin-expressing cells, as markers for astrocytes and early neurons, respectively. This suggests that in the window of early neural differentiation that we study, there is an enhanced generation of progenitor cells rather than a shift in the proportion between neuronal and glial fates. This notion is further supported by the fact that the majority of the BrdU-positive cells were also nestin-positive. This finding is in keeping with a previous report, which showed that constitutive expression of Notch1 ICD in mouse ES cells led to accelerated entry into the neural lineage when ES cells were shifted from ES to N2B27 medium (Lowell et al., 2006).

In conclusion, the data presented here provide insights into a temporal context-dependent output of Notch signaling and identify a temporal window in early neural differentiation of ES cells, in which the cells are susceptible to a Notch-induced, cyclin-D1-dependent increase in proliferation. This may pave the way for a better understanding both of the diversity in the Notch signaling output and of the temporally shifting cell context during early ES cell neural differentiation.

Supplementary materials related to this article can be found online at doi:10.1016/j.ydbio.2010.09.018.

Acknowledgments

We wish to thank Drs. Georg Daley, Raphael Kopan, Michael Kyba, Richard Pestell, Charles Sherr, Shahragim Tajbakhsh, and Jean-Francois Tanti for providing reagents and Susanne Bergstedt for excellent cell culture work. This work was supported by grants to U.L. from the Swedish Foundation for Strategic Research (OBOE), the Swedish Cancer Society, Swedish Brain Power, the Swedish Research Council (DBRM), and the EC projects EuroSystem and NotchIT. H.M. is the recipient of a KID PhD fellowship from Karolinska Institutet. The authors declare no competing financial interests.

References

Almqvist, P.M., Mah, R., Lendahl, U., Jacobsson, B., Hendson, G., 2002. Immunohistochemical detection of nestin in pediatric brain tumors. J. Histochem. Cytochem. 50, 147–158.

Alt, J.R., Cleveland, J.L., Hannink, M., Diehl, J.A., 2000. Phosphorylation-dependent regulation of cyclin D1 nuclear export and cyclin D1-dependent cellular transformation. Genes Dev. 14, 3102–3114.

Bray, S.J., 2006. Notch signalling: a simple pathway becomes complex. Nat. Rev. Mol. Cell Biol. 7, 678–689.

Campa, V.M., Gutierrez-Lanza, R., Cerignoli, F., Diaz-Trelles, R., Nelson, B., Tsuji, T., Barcova, M., Jiang, W., Mercola, M., 2008. Notch activates cell cycle reentry and progression in quiescent cardiomyocytes. J. Cell Biol. 183, 129–141.

Chapman, G., Liu, L., Sahlgren, C., Dahlqvist, C., Lendahl, U., 2006. High levels of Notch signaling down-regulate Numb and Numblike. J. Cell Biol. 175, 535–540.

Dohda, T., Maljukova, A., Liu, L., Heyman, M., Grander, D., Brodin, D., Sangfelt, O., Lendahl, U., 2007. Notch signaling induces SKP2 expression and promotes reduction of p27Kip1 in T-cell acute lymphoblastic leukemia cell lines. Exp. Cell Res. 313, 3141–3152.

Falk, A., Karlsson, T.E., Kurdija, S., Frisen, J., Zupicich, J., 2007. High-throughput identification of genes promoting neuron formation and lineage choice in mouse embryonic stem cells. Stem Cells 25, 1539–1545.

Fu, M., Wang, C., Rao, M., Wu, X., Bouras, T., Zhang, X., Li, Z., Jiao, X., Yang, J., Li, A., Perkins, N.D., Thimmapaya, B., Kung, A.L., Munoz, A., Giordano, A., Lisanti, M.P., Pestell, R.G., 2005. Cyclin D1 represses p300 transactivation through a cyclin-dependent kinase-independent mechanism. J. Biol. Chem. 280, 29728–29742.

Gustafsson, M.V., Zheng, X., Pereira, T., Gradin, K., Jin, S., Lundkvist, J., Ruas, J.L., Poellinger, L., Lendahl, U., Bondesson, M., 2005. Hypoxia requires notch signaling to maintain the undifferentiated cell state. Dev. Cell 9, 617–628.

Hansson, E.M., Stromberg, K., Bergstedt, S., Yu, G., Naslund, J., Lundkvist, J., Lendahl, U., 2005. Aph-1 interacts at the cell surface with proteins in the active gamma-secretase complex and membrane-tethered Notch. J. Neurochem. 92, 1010–1020.

Hansson, E.M., Lanner, F., Das, D., Mutvei, A., Marklund, U., Ericson, J., Farnebo, F., Stumm, G., Stenmark, H., Andersson, E.R., Lendahl, U., 2010. Control of Notch-ligand endocytosis by ligand–receptor interaction. J Cell Sci. 123, 2931–2942.

Hayes, S., Nelson, B.R., Buckingham, B., Reh, T.A., 2007. Notch signaling regulates regeneration in the avian retina. Dev. Biol. 312, 300–311.

Hurlbut, G.D., Kankel, M.W., Lake, R.J., Artavanis-Tsakonas, S., 2007. Crossing paths with Notch in the hyper-network. Curr. Opin. Cell Biol. 19, 166–175.

Karlstrom, H., Bergman, A., Lendahl, U., Naslund, J., Lundkvist, J., 2002. A sensitive and quantitative assay for measuring cleavage of presenilin substrates. J. Biol. Chem. 277, 6763–6766.

Kopan, R., Ilagan, M.X., 2009. The canonical Notch signaling pathway: unfolding the activation mechanism. Cell 137, 216–233.

Kyba, M., Perlingeiro, R.C., Daley, G.Q., 2002. HoxB4 confers definitive lymphoid–myeloid engraftment potential on embryonic stem cell and yolk sac hematopoietic progenitors. Cell 109, 29–37.

Lange, C., Huttner, W.B., Calegari, F., 2009. Cdk4/cyclinD1 overexpression in neural stem cells shortens G1, delays neurogenesis, and promotes the generation and expansion of basal progenitors. Cell Stem Cell 5, 320–331.

Laudon, H., Hansson, E.M., Melen, K., Bergman, A., Farmery, M.R., Winblad, B., Lendahl, U., von Heijne, G., Naslund, J., 2005. A nine-transmembrane domain topology for presenilin 1. J. Biol. Chem. 280, 35352–35360.

Lendahl, U., Lee, K.L., Yang, H., Poellinger, L., 2009. Generating specificity and diversity in the transcriptional response to hypoxia. Nat. Rev. Genet. 10, 821–832.

Leslie, K., Lang, C., Devgan, G., Azare, J., Berishaj, M., Gerald, W., Kim, Y.B., Paz, K., Darnell, J.E., Albanese, C., Sakamaki, T., Pestell, R., Bromberg, J., 2006. Cyclin D1 is transcriptionally regulated by and required for transformation by activated signal transducer and activator of transcription 3. Cancer Res. 66, 2544–2552.

Lindsell, C.E., Boulter, J., diSibio, G., Gossler, A., Weinmaster, G., 1996. Expression patterns of *Jagged*, *Delta1*, *Notch1*, *Notch2*, and *Notch3* genes identify ligand–receptor pairs that may function in neural development. Mol. Cell. Neurosci. 8, 14–27.

Lowell, S., Benchoua, A., Heavey, B., Smith, A.G., 2006. Notch promotes neural lineage entry by pluripotent embryonic stem cells. PLoS Biol. 4, e121.

Marklund, U., Hansson, E. M., Sundstrom, E., de Angelis, M. H., Przemeck, G. K., Lendahl, U., Muhr, J., Ericson, J., 2010. Domain-specific control of neurogenesis achieved through patterned regulation of Notch ligand expression. Development. 137, 437-45.

Mitsiadis, T.A., Henrique, D., Thesleff, I., Lendahl, U., 1997. Mouse Serrate-1 (Jagged-1): expression in the developing tooth is regulated by epithelial–mesenchymal interactions and fibroblast growth factor-4. Development 124, 1473–1483.

Mizutani, K., Yoon, K., Dang, L., Tokunaga, A., Gaiano, N., 2007. Differential Notch signalling distinguishes neural stem cells from intermediate progenitors. Nature 449, 351–355.

Morrison, S.J., Perez, S.E., Qiao, Z., Verdi, J.M., Hicks, C., Weinmaster, G., Anderson, D.J., 2000. Transient Notch activation initiates an irreversible switch from neurogenesis to gliogenesis by neural crest stem cells. Cell 101, 499–510.

Oberg, C., Li, J., Pauley, A., Wolf, E., Gurney, M., Lendahl, U., 2001. The Notch intracellular domain is ubiquitinated and negatively regulated by the mammalian Sel-10 homolog. J. Biol. Chem. 276, 35847–35853.

Peh, G.S., Lang, R.J., Pera, M.F., Hawes, S.M., 2009. CD133 expression by neural progenitors derived from human embryonic stem cells and its use for their prospective isolation. Stem Cells Dev. 18, 269–282.

Poellinger, L., Lendahl, U., 2008. Modulating Notch signaling by pathway-intrinsic and pathway-extrinsic mechanisms. Curr. Opin. Genet. Dev. 18, 449–454.

Ronchini, C., Capobianco, A.J., 2001. Induction of cyclin D1 transcription and CDK2 activity by Notch(ic): implication for cell cycle disruption in transformation by Notch(ic). Mol. Cell. Biol. 21, 5925–5934.

Sahlgren, C., Gustafsson, M.V., Jin, S., Poellinger, L., Lendahl, U., 2008. Notch signaling mediates hypoxia-induced tumor cell migration and invasion. Proc. Natl Acad. Sci. USA 105, 6392–6397.

Stavridis, M.P., Smith, A.G., 2003. Neural differentiation of mouse embryonic stem cells. Biochem. Soc. Trans. 31, 45–49.